Overcoming Performance Limitations of Linear Control with Hybrid Integrator-Gain Systems ⋆

D. van Dinther * B. Sharif * S.J.A.M. van den Eijnden *
H. Nijmeijer * M.F. Heertjes *,** W.P.M.H. Heemels *

* *Department of Mechanical Engineering, Eindhoven University of Technology, The Netherlands (e-mail: d.v.dinther@ tue.nl).*
** *Mechatronics System Design Department, ASML, The Netherlands.*

Abstract: It is well-known that the performance of linear time-invariant (LTI) feedback control is hampered by fundamental limitations. In this paper, it is shown that by using a so-called hybrid integrator-gain system (HIGS) in the controller, important fundamental LTI performance limitations can be overcome. In particular, in this paper, we show this for two well-known limitations, where overshoot in the step-response of the system has to be present for any stabilizing LTI controller. For each case, it is shown that by using HIGS-based control, one can avoid overshoot in the step-response of the system. Key design considerations for HIGS-based controllers as well as the stability of the resulting closed-loop interconnections are discussed.

Keywords: Hybrid integrator-gain systems, Fundamental performance limitations, LTI control.

1. INTRODUCTION

Linear control theory is a well-developed area of research equipped with numerous tools and methods to fit the needs of industry, including tools for the design and synthesis of linear controllers, as well as analysis of the stability and performance thereof. However, all linear time-invariant (LTI) control systems suffer from fundamental limitations such as Bode's gain-phase relationship and the waterbed effect due to Bode's sensitivity integral. These limitations result in well-known design trade-offs in both the frequency- and time-domain (Middleton, 1991). In terms of time-domain performance of LTI systems, restrictions on overshoot, rise time, and settling time of the closed-loop system exist. More specifically, given certain classes of linear systems to be controlled, it is impossible to realize performance beyond particular limits with LTI control, regardless of the choice of the LTI controller. As such, these constraints are called fundamental LTI performance limitations (Seron et al., 1997).

A potential solution to circumvent these limitations is to utilize hybrid or nonlinear control strategies, which by definition are not necessarily bound to the same limitations as LTI systems. Some examples include Variable Gain Control (VGC) (Hunnekens et al., 2016), reset control (Horowitz and Rosenbaum, 1975), switched controllers (Feuer et al., 1997), and more recently the works on hybrid integrator-gain systems (HIGS) (Deenen et al., 2021). In this paper, we will focus on the latter, HIGS, which feature a nonlinear integrator that switches between an integrator- and a gain-mode. This controller was introduced to deal with the classical trade-off in linear control theory between low-frequency disturbance suppression and a desired transient response as typically observed in integral control. The element features an output signal, which has the same sign as its input signal at all times, thereby constantly forcing the output of the system towards the desired setpoint value. In frequency domain, a describing function analysis shows that a HIGS element exhibits similar magnitude characteristics as a linear integrator while inducing only 38.15 degrees of phase lag (see for example van den Eijnden et al. (2020)), as opposed to 90 degrees in the linear case. Similar desirable characteristics are found in the case of reset control elements (Horowitz and Rosenbaum, 1975). However, while reset integrators achieve these properties by producing *discontinuous* control signals, which can potentially excite high-frequency plant, HIGS makes use of *continuous* output signals, making HIGS a powerful control element, especially in high-precision mechatronics, where structural dynamics with numerous weakly damped resonances are encountered.

Multiple studies have shown the possibility of overcoming fundamental time-domain LTI performance limitations by using hybrid control. In particular, in Hunnekens et al. (2016) VGC has been used to overcome one of these limitations. In Beker et al. (2001); Zhao et al. (2019), reset control has been used to overcome three fundamental limitations of LTI control. Recently, in van den Eijnden et al. (2020), it has been shown that a specific time-domain LTI performance limitation can be overcome, by employing a HIGS element. In this paper, the objective is to show that HIGS-based control can, in fact, overcome all the fundamental LTI performance limitations that have been overcome by any other type of nonlinear element, thereby underlining the strength of the HIGS. In the process, we reveal key design considerations for HIGS-based control and discuss the closed-loop stability analysis.

The remainder of this paper is organized as follows. In Section 2, preliminary material related to fundamental limitations of LTI control are given. In Section 3, HIGS and the closed-loop system considered in the paper are described, and the problem statement is provided. Section 4 and Section 5, are concerned with overcoming limitations of LTI control using HIGS-based designs, of which the closed-loop stability will be established in Section 6. Conclusions are stated in Section 7.

⋆ This work is carried out as part of the project "From PID to complex order controller (CLOC)" and is supported by the Netherlands Organization for Scientific Research (NWO) Domain for Applied and Engineering Sciences (TTW).

2. PRELIMINARIES

The sets of reals, integers, and complex values are denoted by $\mathbb{R}$, $\mathbb{Z}$, and $\mathbb{C}$, respectively. Given a vector v, $\|v\|$ denotes its Euclidean norm.

Consider the single-input single-output (SISO) closed-loop interconnection in Fig. 1. Here, the LTI plant and

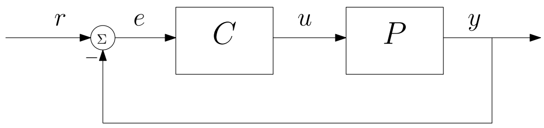

Fig. 1. Linear closed-loop system configuration.

controller are represented by the transfer functions $P(s)$ and $C(s)$, respectively. The plant output $y(t) \in \mathbb{R}$ is subtracted from the reference signal $r(t) \in \mathbb{R}$, generating the error signal $e(t) = r(t) - y(t)$, at time $t \in \mathbb{R}_{\geq 0}$. This error signal is fed to the controller, which in turn generates the control output $u(t) \in \mathbb{R}$, at time $t \in \mathbb{R}_{\geq 0}$.

Assumption 1. *In this work, unless stated otherwise, the reference signal $r(t)$ is assumed to be a unit-step, i.e., $r(t) = 1$ for all $t \in \mathbb{R}_{\geq 0}$. Moreover, it is assumed that the plant P and the controller C have zero initial conditions.*

In Seron et al. (1997) the notion of internal stability (see Definition 2.2.1 in Seron et al. (1997)) is used for stating the limitations of LTI control. However, this definition is only applicable to LTI systems and can not be used to analyze the stability of hybrid closed-loop systems containing HIGS elements. As such, in this work we adopt the notion of Input-to-state stability (ISS) (see Khalil (2002)), which can be used for both LTI and nonlinear systems.

Definition 1. *(Seron et al., 1997) The rise time of the step response of the closed-loop system in Fig. 1 with zero initial conditions (for P and C) is defined as*

$$t_r := \sup_{\delta \in \mathbb{R}_{>0}} \left\{ \delta : y(t) \leq \frac{t}{\delta} \text{ for all } t \in [0, \delta] \right\}. \tag{1}$$

Definition 2. *(Seron et al., 1997) The overshoot of the step response of the closed-loop system in Fig. 1 with zero initial conditions (for P and C), is the maximum value by which the output $y(t)$ exceeds its final setpoint $r(t)$, i.e.,*

$$y_{\text{os}} := \sup_{t \in \mathbb{R}_{\geq 0}} \{-e(t)\}. \tag{2}$$

With the notions of rise time, overshoot, and ISS defined, the fundamental limitations of LTI control considered in this paper can be explicitly stated.

Proposition 1. *(Seron et al., 1997) Consider the closed-loop configuration in Fig. 1. Suppose that the LTI system $P(s)$, is stabilized by the LTI controller $C(s)$. Then*

(i) if $\lim_{s\to 0} sP(s)C(s) = c_1, 0 < |c_1| < \infty$, then

$$\lim_{t\to\infty} e(t) = 0, \text{ and}$$
$$\int_0^\infty e(t)\,\mathrm{d}t = \frac{1}{c_1};$$

(ii) if $\lim_{s\to 0} s^2 P(s)C(s) = c_2, 0 < |c_2| < \infty$, then

$$\lim_{t\to\infty} e(t) = 0, \text{ and} \tag{3}$$
$$\int_0^\infty e(t)\,\mathrm{d}t = 0. \tag{4}$$

Proof. See Seron et al. (1997), Section 1.3. □

Remark 1. *In the closed-loop interconnection of Fig. 1, when the transfer function $P(s)C(s)$ has a single open-loop integrator, item (i) of Proposition 1 holds. This does not necessarily imply that the step response $y(t) = 1 - e(t)$, overshoots. However, as shown in Proposition 1 of Beker et al. (2001), if the rise time t_r is sufficiently slow such that $t_r > \frac{2}{c_1}$, the unit-step response $y(t)$ overshoots, for any stabilizing LTI controller $C(s)$.*

Remark 2. *In the closed-loop interconnection of Fig. 1, the error signal $e(t)$ will be initially positive. Indeed for $y(t_0) = 0$, one has $e(t_0) = 1 - y(t_0) = 1$. If $P(s)C(s)$ has two open-loop integrators, due to (4) in Proposition 1, the error $e(t)$ will have a change of sign. This implies that there has to be overshoot in the step-response $y(t)$ for any stabilizing LTI controller $C(s)$. Moreover, it is easy to show that (4) also holds when $P(s)C(s)$ contains more than two integrators. Thus, for an open-loop plant containing two or more open-loop integrators, a non-zero overshoot is unavoidable in the step-response $y(t)$ for any stabilizing LTI controller $C(s)$.*

Remark 3. *As shown in Seron et al. (1997), if the plant has an open-loop pole p in the right-half complex plane such that $\mathrm{Im}(p) = 0$, the unit-step response $y(t)$ necessarily overshoots for any internally stabilizing LTI controller $C(s)$. Moreover the overshoot satisfies*

$$y_{\text{os}} \geq \frac{(pt_r - 1)e^{pt_r} + 1}{pt_r} \geq \frac{pt_r}{2}, \tag{5}$$

where t_r is the rise time as defined in (1).

The limitations described in Remark 1, 2, and 3 have been shown to be overcome by hybrid and nonlinear control strategies such as VGC and reset control. In van den Eijnden et al. (2020) a HIGS-based design is presented that overcomes the limitation in Remark 3. The aim of this paper is to show that by using HIGS-based control, the limitations of LTI control in Remarks 1, and 2 can also be overcome, thereby showing that HIGS-based control can overcome all the limitations that have been previously overcome by other control strategies.

3. SYSTEM DESCRIPTION AND PROBLEM STATEMENT

3.1 Hybrid integrator-gain systems

The hybrid integrator-gain system (HIGS), denoted by $\mathscr{H}$, is a discontinuous piecewise linear (PWL) system

$$\mathscr{H} : \begin{cases} \dot{x}_h(t) = \omega_h z(t) & \text{if } (z(t), u(t), \dot{z}(t)) \in \mathscr{F}_1, & \text{(6a)} \\ x_h(t) = k_h z(t) & \text{if } (z(t), u(t), \dot{z}(t)) \in \mathscr{F}_2, & \text{(6b)} \\ u(t) = x_h(t), & & \text{(6c)} \end{cases}$$

with state $x_h(t) \in \mathbb{R}$, input $z(t) \in \mathbb{R}$, time-derivative of input $\dot{z}(t) \in \mathbb{R}$, and output $u(t) \in \mathbb{R}$, at time $t \in \mathbb{R}_{\geq 0}$. The parameters $\omega_h \in [0, \infty)$ and $k_h \in (0, \infty)$ denote the integrator frequency and gain value, respectively. Moreover, $\mathscr{F}_1$ and $\mathscr{F}_2$ denote the regions in $\mathbb{R}^3$ where the different subsystems are active. The HIGS is designed to primarily operate in the so-called integrator mode given by (6a). The integrator-mode dynamics can be followed as long as the input-output pair (z, u) of $\mathscr{H}$ remain inside the sector

$$\mathscr{F} := \left\{ (z, u, \dot{z}) \in \mathbb{R}^3 \mid zu \geq \frac{1}{k_h} u^2 \right\}. \tag{7}$$

When the input-output pair (z, u) tends to leave $\mathscr{F}$, a switch is made to the so-called gain mode as given by (6b), so that the trajectories move along the sector boundary where $z = k_h u$ and thus remain in $\mathscr{F}$. As such, the sets $\mathscr{F}_1$ and $\mathscr{F}_2$ are given by

$$\mathscr{F}_1 := \mathscr{F} \setminus \mathscr{F}_2, \tag{8}$$

$$\mathscr{F}_2 := \left\{(z, u, \dot{z}) \in \mathbb{R}^3 \mid u = k_h z \wedge \omega_h z^2 > k_h \dot{z} z\right\}. \tag{9}$$

As a result of this construction, the input and output of a HIGS element have the same sign at all times. It is assumed that the initial condition of the HIGS is chosen as $x_h(0) = 0$. The interested reader is referred to Deenen et al. (2021); Sharif et al. (2019), for a proof of existence and forward completeness of Carathéodory solutions as well as stability analysis of HIGS-controlled systems.

3.2 Closed-loop system description

We consider the closed-loop interconnection in Fig. 2, where, as before, the LTI plant to be controlled has

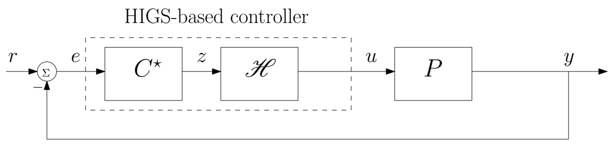

Fig. 2. Closed-loop system configuration with HIGS-element.

transfer function $P(s)$. In contrast with the closed-loop interconnection in Fig. 1, the LTI controller has been replaced with a HIGS-based controller consisting of a HIGS element $\mathscr{H}$ as in (6) and an LTI controller with transfer function $C^\star(s)$. The state-space realization of $P(s)$ is given by

$$\Sigma_p : \begin{cases} \dot{x}_p(t) = A_p x_p(t) + B_p u(t), \\ y(t) = C_p x_p(t), \end{cases} \tag{10}$$

where $x_p(t) \in \mathbb{R}^{n_p}$ is its state-vector, $u(t) \in \mathbb{R}$ is the input to the plant, $y(t) \in \mathbb{R}$ is the plant output at time $t \in \mathbb{R}_{\geq 0}$, and A_p, B_p, C_p are matrices of appropriate dimensions. Furthermore, the initial condition $x_p(0)$, is assumed to be zero. Similarly, let $(A_{C^\star}, B_{C^\star}, C_{C^\star}, D_{C^\star})$, be a state-space realization of $C^\star(s)$. Due to the piecewise linear (PWL) nature of the HIGS, the closed-loop interconnection can be represented as

$$\Sigma : \begin{cases} \dot{x} = A_i x + B_i w, & \text{if } (z, u, \dot{z}) \in \mathscr{F}_i, i \in \{1, 2\}, \\ y = Cx, \end{cases} \tag{11}$$

with state vector $x(t) = [x_p(t)^\top, x_{C^\star}(t)^\top, x_h(t)]^\top \in \mathbb{R}^n$, where x_p, $x_{C^\star}$, and x_h, denote the state of $P(s)$, $C^\star(s)$, and $\mathscr{H}$, respectively. Moreover, the performance output is denoted by $y(t)$, and $w(t) = [r(t)^\top, \dot{r}(t)^\top]^\top$ represents the vector of exogenous inputs. In addition, $\mathscr{F}_i, i \in \{1, 2\}$, denote the regions where integrator-mode and gain-mode dynamics are active, respectively. The representation (11), will prove useful for stability analysis of the closed-loop systems considered in the following sections.

3.3 Problem formulation

The objective of this work is to design HIGS-based controllers overcoming the LTI performance limitations presented in Remark 1 and Remark 2. For each case, a HIGS-based design as in Fig. 2 is presented, that (i) achieves zero steady-state tracking error (as a linear integrator would) while (ii) eliminating overshoot and (iii) stabilizing the closed-loop system, thereby realizing objectives that are impossible to achieve with any LTI controller.

4. SINGLE OPEN-LOOP INTEGRATOR WITHOUT OVERSHOOT

Consider the interconnection in Fig. 2 with $P(s) = 1/s$, $C^\star(s) = 1$. As explained in Remark 1, for this choice of $P(s)$, the unit-step response of the system necessarily overshoots for any stabilizing LTI controller satisfying item (i) of Proposition 1, if the rise time t_r is sufficiently slow. More specifically, the step response overshoots if $t_r > 2/c_1$ with c_1 as defined in item (i) of Proposition 1. For determining the constant c_1 we use the fact that the steady-state error of the closed-loop system to a unit-ramp input, i.e., $r(t) = t$, is given by $\lim_{t\to\infty} e_{\text{ramp}}(t) := \frac{1}{c_1}$, where e_{ramp} denotes the error signal to a unit-ramp input. Indeed, by application of the final value theorem to the closed-loop system in Fig. 1, the steady-state error to a unit-ramp input is found to be

$$\lim_{t\to\infty} e_{\text{ramp}}(t) = \lim_{s\to 0} \frac{1}{s + sP(s)C(s)}. \tag{12}$$

Due to item (i) of Proposition 1, $\lim_{s\to 0} sP(s)C(s) = c_1$ and thus, for (12) we obtain $\lim_{s\to 0} \frac{1}{s+sP(s)C(s)} = \frac{1}{c_1}$. For a HIGS-based design to overcome the limitation in Remark 1, it should achieve the same steady-state error to a unit-ramp input and a step response with a rise time satisfying $t_r > 2/c_1$, without any overshoot. Thus, we start by computing the tracking error to a unit-ramp input for the closed-loop interconnection of $P(s)$ and a single HIGS element, in order to compute the amount of rise time necessary for having overshoot with any LTI controller. The error signal can be computed to be

$$e_{\text{ramp}}(t) = \begin{cases} \dfrac{1}{\sqrt{\omega_h}} \sin(\sqrt{\omega_h} t), & t \in [0, t_s), \\ \dfrac{1}{k_h} + \left(\dfrac{1}{\sqrt{\omega_h}} \sin(\sqrt{\omega_h} t_s) - \dfrac{1}{k_h}\right) e^{-k_h(t-t_s)}, & t \geq t_s, \end{cases} \tag{13}$$

where ω_h and k_h denote the integrator frequency and the gain parameter of the HIGS element, respectively. Moreover, $t_s = \frac{2}{\sqrt{\omega_h}} \arctan\left(\frac{k_h}{\sqrt{\omega_h}}\right)$ is the time instant when the HIGS switches from the integrator mode to gain mode. To see how (13) is derived, let us first note that for zero initial conditions the HIGS element $\mathscr{H}$ starts to operate in the integrator mode wherein the dynamics are given by the transfer function $\mathscr{H}_i(s) = \omega_h/s$, leading to the expression

$$E_{\text{ramp}}(s) = \frac{R(s)}{1 + \mathscr{H}_i(s)P(s)} = \frac{1/s^2}{1 + \omega_h/s^2} = \frac{1}{s^2 + \omega_h}, \tag{14}$$

for the error, in the complex domain. Here, $E_{\text{ramp}}(s)$ and $R(s)$ denote the Laplace transforms of the error $e_{\text{ramp}}(t)$ and the reference $r(t)$, respectively. By applying the inverse Laplace transform to (14) we obtain

$$e_{\text{ramp}}(t) = \frac{1}{\sqrt{\omega_h}} \sin(\sqrt{\omega_h} t), \quad \forall t \in [0, t_s). \tag{15}$$

To determine t_s, note that at $t = t_s$, $k_h e_{\text{ramp}}(t_s) = u(t_s)$, and $\omega_h e_{\text{ramp}}(t_s) > k_h \dot{e}_{\text{ramp}}(t_s)$, such that at this time instant operation in the integrator mode leads to violation of the sector constraint of the HIGS. Thus one has

$$\begin{aligned} u(t_s) &= \int_0^{t_s} \omega_h e_{\text{ramp}}(t) dt = 1 - \cos(\sqrt{\omega_h} t_s) \\ &= k_h e_{\text{ramp}}(t_s) = \frac{k_h}{\sqrt{\omega_h}} \sin(\sqrt{\omega_h} t_s), \end{aligned} \tag{16}$$

where the last equality follows from (15). By solving (16) we obtain $t_s = \frac{2}{\sqrt{\omega_h}} \left(\arctan\left(\frac{k_h}{\sqrt{\omega_h}}\right)\right)$. Note that by using this expression for t_s together with (15), one can confirm that the condition $\omega_h e_{\text{ramp}}(t_s) > k_h \dot{e}_{\text{ramp}}(t_s)$ is satisfied and thus, a switch to the gain mode dynamics is indeed required at $t = t_s$. Upon switching to the gain mode, the dynamics of the HIGS element are given by the transfer function $\mathscr{H}_g(s) = k_h$. To derive the expression for $e_{\text{ramp}}(t)$ after the switching instance $t = t_s$, we define a shifted time parameter $t' = t - t_s$, and a shifted input $r(t') = t' + e(t_s) = t' + \frac{1}{\sqrt{\omega_h}} \sin(\sqrt{\omega_h} t_s)$, for all $t' \in \mathbb{R}_{\geq 0}$. When the HIGS operates in the gain mode, we obtain the following expression for the error signal in the complex domain by application of the Laplace transform to $r(t')$ and using the same reasoning as in (14),

$$E_{\text{ramp}}(s) = \frac{R(s)}{1 + \mathscr{H}_g(s)P(s)} \tag{17}$$

$$= \frac{1}{k_h}\frac{1}{s} + \left(\frac{1}{\sqrt{\omega_h}} \sin(\sqrt{\omega_h} t_s) - \frac{1}{k_h}\right) \frac{1}{s + k_h}.$$

Application of the inverse Laplace transform to (17) gives

$$e(t') = \mathscr{L}^{-1}\{E\}(t') \tag{18}$$

$$= \frac{1}{k_h} + \left(\frac{1}{\sqrt{\omega_h}} \sin(\sqrt{\omega_h} t_s) - \frac{1}{k_h}\right) e^{-k_h t'}.$$

Using (18), one verifies $\omega_h e(t') \geq k_h \dot{e}(t')$, for all $t' \in \mathbb{R}_{\geq 0}$, $w_h > 0$, and $k_h > 0$. Hence, after $t = t_s$, no switch is made back to the integrator mode. By substituting $t' = t - t_s$ in (18), one obtains the second expression in (13) for $t \geq t_s$. Building on the discussion above, the constant c_1 is given by $c_1 = \frac{1}{\lim_{t\to\infty} e_{\text{ramp}}(t)} = k_h$. As such, due to Remark 1, if we find a combination of k_h and ω_h such that the closed-loop system's step response does not overshoot and its rise time satisfies $t_r > 2/k_h$, we have overcome the limitation under consideration. To determine whether the step response of the closed-loop interconnection of $P(s)$ and a single HIGS element overshoots, we proceed by computing the error signal to a unit-step input, i.e., $r(t) = 1$, given by

$$e_{\text{step}}(t) = \begin{cases} \cos(\sqrt{\omega_h} t), & t \in [0, t_s), \\ \cos(\sqrt{\omega_h} t_s) e^{-k_h(t - t_s)}, & t \geq t_s, \end{cases} \tag{19}$$

where the switching time is given by $t_s = \frac{1}{\sqrt{\omega_h}} \arctan\left(\frac{k_h}{\sqrt{\omega_h}}\right)$. The derivation of (19) follows the same methodology used in the derivation of (13) and is not included here due to space limitations. Clearly the unit-step response of the system never overshoots, if $e_{\text{step}}(t)$ is non-negative for all $t \in \mathbb{R}_{\geq 0}$. Note that for e_{step} to be non-negative at all times, it is necessary that $\cos(\sqrt{\omega_h} t)$ is non-negative for all $t \in [0, t_s]$. Using the expression for t_s, this condition is equivalent to $\arctan\left(\frac{k_h}{\sqrt{\omega_h}}\right) \leq \frac{\pi}{2}$, which is always satisfied since $\frac{-\pi}{2} < \arctan(\cdot) < \frac{\pi}{2}$. Moreover, for $t \geq t_s$, since $\cos(\sqrt{\omega_h} t_s) \geq 0$ and $k_h > 0$, it holds that $0 \leq \cos(\sqrt{\omega_h} t_s) e^{-k_h(t - t_s)} \leq \cos(\sqrt{\omega_h} t_s)$. Thus we conclude that $e_{\text{step}}(t) \geq 0$, for all $t \geq 0$ and therefore the unit-step response $y_{\text{step}}(t) = 1 - e_{\text{step}}(t)$ never overshoots, regardless of the choice of $\omega_h > 0$ and $k_h > 0$. Additionally, note that $\lim_{t\to\infty} e_{\text{step}}(t) = 0$, such that a steady-state tracking error of zero is achieved.

It remains to show that it is possible to find a combination of the parameters ω_h and k_h, such that the constraint on the rise time, i.e., $t_r > 2/c_1 = 2/k_h$, is satisfied. Based on Definition 1, the rise time t_r is determined from tangency of the step response $y(t) = 1 - e_{\text{step}}(t)$, with the line $\hat{y}(t) := t/t_r$. Thus, we seek the pair $(t^\star, t_r)$, $t^\star > 0$, such that

$$y(t^\star) = \hat{y}(t^\star), \quad \dot{y}(t^\star) = \dot{\hat{y}}(t^\star). \tag{20}$$

With $k_h = 1.5$, $\omega_h = 0.25$, using (20) gives $t_r \approx 2.8 > \frac{2}{k_h}$. Hence, we have found a combination of k_h and ω_h which lead to no overshoot in the step response $y(t)$ while respecting the constraint $t_r > 2/k_h$.

Remark 4. *ISS of the closed-loop system considered in this section will be established in Section 6.*

The analysis presented thus far is verified with the simulation results in Fig. 3. As it can be seen in Fig. 3, a zero steady-state tracking error is achieved. Moreover, there is no overshoot in the step response $y(t)$, and the constraint on the rise time of the step response is satisfied.

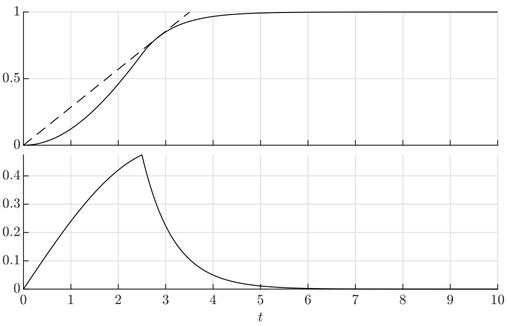

Fig. 3. Step response $y(t)$ and control output $u(t)$ for the closed-loop system configuration with HIGS-based control and one open-loop integrator. The dashed line indicates the rise-time line $\hat{y}(t) = t/t_r$.

5. MULTIPLE OPEN-LOOP INTEGRATORS WITHOUT OVERSHOOT

Consider the interconnection in Fig. 2 with $P(s) = (0.05s + 1)/s^2$. As explained in Remark 2, when the reference signal $r(t)$ is a unit-step, for this choice of $P(s)$ the step response of the system necessarily overshoots. In order to overcome this limitation, a stabilizing HIGS-based design that achieves a zero steady-state tracking error to a unit-step reference, while leading to a error signal $e(t)$, which is non-negative for all time $t \in \mathbb{R}_{\geq 0}$, is desired. Achieving the latter objective results in a step response with no overshoot.

The plant $P(s)$ is assumed to have zero initial conditions. As such, a positive initial control signal $u(t)$ is required to steer the output of the system towards the setpoint. Moreover, note that $P(s) = 1/s^2 + 0.05/s$, with the double integrator $1/s^2$, the more dominant term. As such, the system dominantly behaves as a double integrator (described by $\ddot{y}(t) = u(t)$). As a result, when the output $y(t)$ approaches the setpoint value, a sign change in the control input $u(t)$ is needed in order to decrease $\dot{y}(t)$, so that overshoot is avoided and a zero steady-state tracking error is achieved. However, $u(t)$ is the output of the HIGS element and as explained in Section 3.1, the input and output of a HIGS element always have the same sign. Thus, if the error signal $e(t)$ is fed into the HIGS element, a sign change in $u(t)$ results in a change of sign in $e(t)$ which in turn, would lead to overshoot in the step response $y(t)$. To address this problem, we propose to place an LTI controller, denoted by $C^\star(s)$ in Fig 2, in front of the HIGS-element. In particular, $C^\star(s)$ is the PD filter

$$C^\star(s) = k_p \left(\frac{s}{\omega_c} + 1\right), \tag{21}$$

where $\omega_c = |1 + 4j/\pi|\omega_h/k_h$ is the cross-over frequency of the describing function of a HIGS-element (see van den

Eijnden et al. (2020), for an explicit expression of the describing function of the HIGS). By filtering the error signal with $C^{\star}(s)$ prior to feeding it to the HIGS element, the input to the HIGS becomes

$$z(t) = k_p \left(e(t) + \frac{\dot{e}(t)}{\omega_c} \right). \tag{22}$$

With this choice of $C^{\star}(s)$, it is possible to have a sign change in the input $z(t)$ to the HIGS, while avoiding change of sign in $e(t)$. From (22) one has $z(t) < 0$, if

$$\dot{e}(t) < -\omega_c e(t). \tag{23}$$

Hence, including the linear filter $C^{\star}(s)$ provides the possibility of changing the sign of the control signal $u(t)$, while avoiding a change of sign in $e(t)$. Therefore, by using (23) as a tuning guideline, a suitable value of ω_c (which can be tuned by changing the value of ω_h) can be obtained, which in turn leads to a control signal generated by the HIGS element that is initially positive and drives the system's output towards the setpoint value. At points when (23) holds true, the HIGS element changes the sign of its output, thereby slowing down the system's response and thus potentially avoiding overshoot. As such, it is clear that the choice of ω_c (and thus ω_h) is crucial in the design of the HIGS-based controller. In particular, a suitable value of ω_h would lead to a change of sign in $u(t)$, fast enough to avoid overshoot. On the other hand, a too high ω_h value would result in a step response with overshoot. Indeed for $\omega_h \to \infty$, one has $z(t) \to k_p e(t)$. Therefore, as $\omega_h \to \infty$ a sign change in $z(t)$ implies a change of sign in $e(t)$ leading to overshoot. The unit-step response of the closed-loop system where the controller parameters are chosen as, $k_h = 1$, $\omega_h = 0.5$, and $k_p = 10$, is portrayed in Fig. 4. As it can be seen in Fig. 4, the step response y

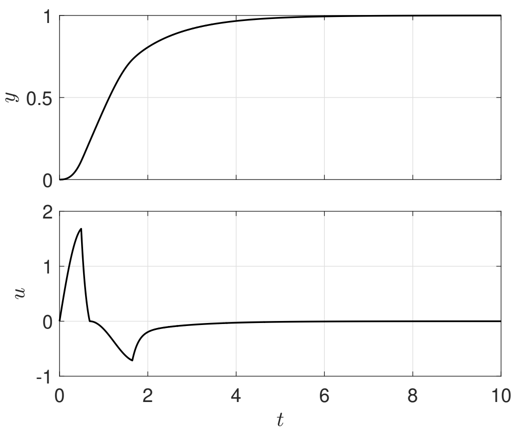

Fig. 4. Step response $y(t)$ and control output $u(t)$ for the closed-loop system configuration with HIGS-based control and two open-loop integrators.

does not overshoot and a zero steady-state tracking error is achieved. Further insights into the mechanism leading to the absence of overshoot can be obtained by investigating the trajectories in Fig. 5. As shown in Fig. 5, the HIGS input $z(t)$ and output $u(t)$ show a change in sign, while $e(t) \geq 0$ for all $t \geq 0$. In particular, as shown in Fig. 5a, the HIGS initially operates in integrator-mode. After some time, a switch is made to the gain-mode dynamics, resulting in trajectories that move towards the origin of the (z, u) plane. The operation of the HIGS in the gain-mode leads to trajectories in the $(e, \dot{e})$ plane that cross the line $\dot{e} = -\omega_c e$ (see Fig. 5b), such that (23) holds and thus results in a sign change in $z(t)$. After this point, the

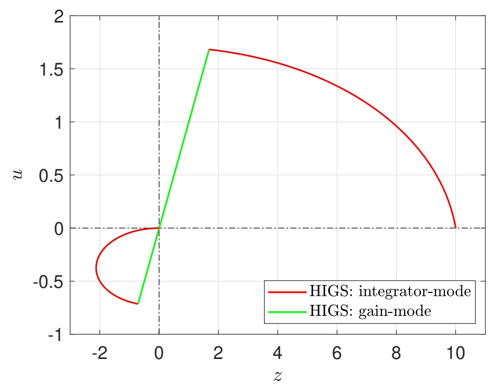

(a) HIGS input $z(t)$ versus HIGS output $u(t)$

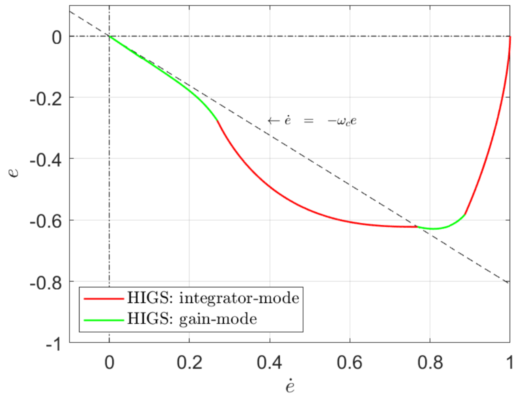

(b) Error $e(t)$ versus its derivative $\dot{e}(t)$

Fig. 5. Trajectories of the HIGS-controlled system with two open-loop integrators.

trajectories in the $(e, \dot{e})$ plane eventually move towards the line $\dot{e} = -\omega_c e$, intersect it at the point $e = \dot{e} = 0$, and remain there. This leads to a steady-state error of zero without any overshoot in the step response.

The results presented in this section suggest that by using HIGS-based control, the limitation stated in Remark 2 can be overcome. In order to complete this claim, it remains to show that the closed-loop system is ISS. This will be done in Section 6.

6. CLOSED-LOOP STABILITY

In order to complete the claim that the fundamental limitations considered in Remark 1 and Remark 2 are overcome, ISS of the closed-loop systems considered in Section 4 and Section 5 has to be established. Recall the general HIGS-controlled system in Fig. 2, described by piecewise linear representation (11) with state vector $x(t) = [x_p(t)^{\top} x_{C^{\star}}(t)^{\top} x_h(t)]^{\top} \in \mathbb{R}^n$. The matrices $A_i, B_i, i \in \{1, 2\}$ are given in (24), (25), (on the last page) where $(A_q, B_q, C_q, D_q), q \in \{P, C^{\star}\}$, denote the state-space matrices defined in Section 3. Moreover, the output matrix in (11), is given by $C = [C_p \; 0 \; 0]$. In order to verify ISS of the closed-loop system (11), we employ the results in Theorem 1 of van den Eijnden et al. (2019). To this end, let us define a matrix E such that $Ex = [z \; u, \dot{z}]^{\top}$ and consider the LMIs

$$P - S^{\top} W S \succ 0, \tag{26}$$

$$A_1^{\top} P + P A_1 + S^{\top} U S \prec 0, \tag{27}$$

$$A_2^{\top} P + P A_2 + \Gamma G + G^{\top} \Gamma^{\top} + Z^{\top} V Z \prec 0, \tag{28}$$

$$A_1 = \begin{bmatrix} A_p & 0 & B_p \\ -B_{C^\star} C_p & A_{C^\star} & 0 \\ -\omega_h D_{C^\star} C_p & \omega_h C_{C^\star} & 0 \end{bmatrix}, \quad B_1 = \begin{bmatrix} 0 & 0 \\ B_{C^\star} & 0 \\ \omega_h D_{C^\star} & 0 \end{bmatrix}, \tag{24}$$

$$A_2 = \begin{bmatrix} A_p & 0 & B_p \\ -B_{C^\star} C_p & A_{C^\star} & 0 \\ (-k_h C_{C^\star} B_{C^\star} C_p - k_h D_{C^\star} C_p A_p) & k_h C_{C^\star} A_{C^\star} & -k_h D_{C^\star} C_p B_p \end{bmatrix}, \quad B_2 = \begin{bmatrix} 0 & 0 \\ B_{C^\star} & 0 \\ k_h C_{C^\star} B_{C^\star} & k_h D_{C^\star} \end{bmatrix}. \tag{25}$$

where $P = P^\top$. Moreover, W, V, and U are symmetric matrices with non-negative entries, and Γ is a real vector. The matrices S and Z are given by

$$S = \begin{bmatrix} 1 & 0 \\ k_h & 1 \end{bmatrix}^{-1} \begin{bmatrix} 1 & 0 & 0 \\ 0 & 1 & 0 \end{bmatrix} E, \quad z = \begin{bmatrix} -k_h & \omega_h \\ 0 & 1 \end{bmatrix} \begin{bmatrix} 0 & 0 & 1 \\ 1 & 0 & 0 \end{bmatrix} E.$$

Additionally, $G = LE$, with $L = [k_h \ \ -1 \ \ 0]$. For details on the rationale behind the choice of the above matrices see van den Eijnden et al. (2019). As shown in van den Eijnden et al. (2019), the feasibility of the above LMIs, guarantee the existence of a common Lyapunov function $V(x) = x^\top P x$ and thus prove exponential stability of the closed-loop system, with the exogenous input $w = 0$. In particular, (26) ensures the positive definiteness of $V(x)$, within the input-output space of the HIGS. Moreover, feasibility of (27) implies that $V(x)$ is decreasing along the trajectories of the system in the integrator mode. Lastly (28), implies that $V(x)$ decreases along the system trajectories in the gain mode. Here, use has been made of S-procedure relaxations as well as Finsler's lemma (see for example van den Eijnden et al. (2019)) to reduce the conservatism associate with the LMI conditions. Next, using the fact that w is an affine input to (11), one can utilize the same arguments as in Khalil (2002), Section 4.9, to show that $V(x)$ is an ISS-Lyapunov function for (11) and thus, the system is ISS with respect to all bounded exogenous inputs w. The above stability analysis procedure has been applied to the closed-loop systems considered in Section 4 and Section 5, i.e., (11), where the matrices in (24) and (25) are computed based on the parameters specified in these sections. For solving the LMIs, use has been made of the MATLAB toolbox `Yalmip` and the solver `MOSEK`. For the example in Section 4, a feasible solution with

$$P = \begin{bmatrix} 0.2521 & 0.3592 \\ 0.3592 & 0.8331 \end{bmatrix}, \ W = \begin{bmatrix} 3.264 & 1.04 \\ 1.04 & 0.7449 \end{bmatrix},$$
$$U = \begin{bmatrix} 0.6017 & 3.647 \\ 3.647 & 0.72 \end{bmatrix}, \ V = \begin{bmatrix} 0.5641 & 0.5501 \\ 0.5501 & 1.038 \end{bmatrix},$$
$$\Gamma = [\, 0.0472 \ \ -0.2521 \,].$$

is found for the LMIs. Moreover for the system considered in Section 5, the LMIs are rendered feasible with

$$P = \begin{bmatrix} 6863.0 & 1092.0 & 7617.0 & 4259.0 \\ 1092.0 & 644.3 & -881.7 & 1048.0 \\ 7617.0 & -881.7 & 20999.0 & 3833.0 \\ 4259.0 & 1048.0 & 3833.0 & 3569.0 \end{bmatrix}, W = \begin{bmatrix} 53.15 & 97.99 \\ 97.99 & 84.31 \end{bmatrix}$$

$$U = \begin{bmatrix} 13.0 & 12433.0 \\ 12433.0 & 195.4 \end{bmatrix}, \ V = \begin{bmatrix} 3.064 & 5593.0 \\ 5593.0 & 4.902\,10^6 \end{bmatrix},$$

$$\Gamma = [\, -5.428\,10^6 \ \ -2.457\,10^6 \ \ -5.058\,10^6 \ \ 1.019\,10^7 \,].$$

As a result of the feasibility of the LMIs, we conclude ISS of the closed-loop systems in Section 4 and Section 5. As such, we claim that the HIGS-based designs proposed in the previous sections overcome the fundamental limitations of LTI control, described in Remarks 1 and 2.

7. CONCLUSION

In this paper, we have employed HIGS-based control for overcoming two well-known fundamental time-domain performance limitations of LTI control. In particular, we have shown that by using HIGS-based control, fundamental overshoot limitations inherent to LTI systems with one or multiple open-loop integrators can be overcome. This shows that all limitations of LTI control that have been previously overcome by nonlinear and hybrid control strategies, can also be overcome by HIGS-based control. Future research directions include the extension of the results presented in this paper to more complex and industrially relevant examples. Additionally, systematic procedures for design of HIGS-based controllers that overcome fundamental performance limitations are of interest.

REFERENCES

Beker, O., Hollot, C.V., and Chait, Y. (2001). Plant with integrator: an example of reset control overcoming limitations of linear feedback. *IEEE Transactions on Automatic Control*, 46(11), 1797–1799. doi:10.1109/9.964694.

Deenen, D., Sharif, B., van den Eijnden, S., Nijmeijer, H., Heemels, W., and Heertjes, M. (2021). Projection-Based Integrators for Improved Motion Control: Formalization, Well-posedness and Stability of Hybrid Integrator-Gain Systems. *Provissionally accepted in Automatica.*

Feuer, A., Goodwin, G.C., and Salgado, M. (1997). Potential benefits of hybrid control for linear time invariant plants. *Proceedings of the 1997 American Control Conference*, 5, 2790–2794. doi:10.1109/ACC.1997.611964.

Horowitz, I. and Rosenbaum, P. (1975). Non-linear design for cost of feedback reduction in systems with large parameter uncertainty. *International Journal of Control*, 21(6), 977–1001. doi:10.1080/00207177508922051.

Hunnekens, B.G.B., van de Wouw, N., and Nešić, D. (2016). Overcoming a fundamental time-domain performance limitation by nonlinear control. *Automatica*, 67, 277–281. doi:10.1016/j.automatica.2016.01.021.

Khalil, H.K. (2002). *Nonlinear Systems.* Prentice Hall, third edition.

Middleton, R.H. (1991). Trade-offs in linear control system design. *Automatica*, 27(2), 281–292. doi:10.1016/0005-1098(91)90077-F.

Seron, M.M., Braslavsky, J.H., and Goodwin, G.C. (1997). *Fundamental Limitations in Filtering and Control.* Springer, London. doi:10.1007/978-1-4471-0965-5.

Sharif, B., Heertjes, M.F., and Heemels, W.P.M.H. (2019). Extended Projected Dynamical Systems with Applications to Hybrid Integrator-Gain Systems. In *2019 IEEE Conference on Decision and Control (CDC).* IEEE.

van den Eijnden, S.J.A.M., Heertjes, M.F., Heemels, W.P.M.H., and Nijmeijer, H. (2020). Hybrid Integrator-Gain Systems: A Remedy for Overshoot Limitations in Linear Control? *IEEE Control Systems Letters.*

van den Eijnden, S., Heertjes, M., and Nijmeijer, H. (2019). Robust stability and nonlinear loop-shaping design for hybrid integrator-gain-based control systems. In *2019 American Control Conference, ACC 2019*, 3063–3068. Institute of Electrical and Electronics Engineers, United States.

Zhao, G., Nešić, D., Tan, Y., and Hua, C. (2019). Overcoming overshoot performance limitations of linear systems with reset control. *Automatica*, 101, 27–35. doi: https://doi.org/10.1016/j.automatica.2018.11.038.